

1
2
3
4
5
6
7
8
9
10
11
12
13
14
15
16
17
18
19
20
21
22
23
24
25
26
27
28
29
30
31
32
33
34
35
36
37
38
39
40
41
42
43
44
45
46
47
48
49
50
51
52
53
54
55
56
57
58
59
60

Temperature Driven Changeover in the Electron Transfer Mechanism of a Thermophilic Plastocyanin

José Luis Olloqui-Sariego[§], Blas Moreno-Beltrán[‡], Antonio Díaz-Quintana[‡], Miguel A. De la Rosa[‡], Juan José Calvente[§] and Rafael Andreu[§]*

[§]Departamento de Química Física. Universidad de Sevilla. c/ Profesor García González, 1. 41012 Sevilla (Spain).

[‡]Instituto de Bioquímica Vegetal y Fotosíntesis, cicCartuja. Universidad de Sevilla y C.S.I.C. Avd. Américo Vespucio 49. 41092 Sevilla (Spain)

AUTHOR INFORMATION

Corresponding Author

E-mail: jlolloqui@us.es

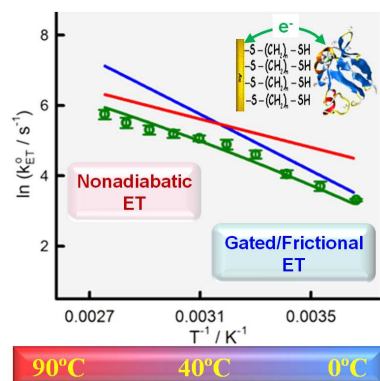
Departamento de Química Física. Universidad de Sevilla.

c/ Profesor García González, 1. 41012 Sevilla. Spain

1
2
3
4
5
6
7
8
9
10
11
12
13
14
15
16
17
18
19
20
21
22
23
24
25
26
27
28
29
30
31
32
33
34
35
36
37
38
39
40
41
42
43
44
45
46
47
48
49
50
51
52
53
54
55
56
57
58
59
60

ABSTRACT. Electron transfer kinetics of the thermophilic protein Plastocyanin from *Phormidium laminosum* adsorbed on 1, ω -alkanedithiol self-assembled monolayers (SAMs) deposited on gold have been investigated. The standard electron transfer rate constant has been determined as a function of electrode-protein distance and solution viscosity over a broad temperature range (0 – 90 °C). For either thin or thick SAMs, the electron transfer regime remains invariant with temperature; whereas for the 1,11-undecanethiol SAM of intermediate chain-length, a kinetic regime changeover from a gated or friction-controlled mechanism at low temperature (0 - 30° C) to a non-adiabatic mechanism above 40 °C is observed. To the best of our knowledge, this is the first time a thermal-induced transition between these two kinetic regimes is reported for a metalloprotein.

TOC GRAPHICS



50
51
52
53
54
55
56
57
58
59
60

KEYWORDS. Thermophilic plastocyanin; protein electron transfer; kinetic regime changeover; 1, ω -alkanedithiol monolayer; temperature; solution viscosity.

1
2
3
4
5
6
7
8
9
10
11
12
13
14
15
16
17
18
19
20
21
22
23
24
25
26
27
28
29
30
31
32
33
34
35
36
37
38
39
40
41
42
43
44
45
46
47
48
49
50
51
52
53
54
55
56
57
58
59
60

Several strategies have been proposed to elucidate the factors that determine the rate of electron exchange between proteins and electrodes. Among them stand out the analysis of the effects of protein-electrode distance, temperature or solution viscosity on the electron transfer (ET) rate constant.¹⁻⁵ These studies have revealed two distinct kinetic regimes, in which ET rates are either independent or exponentially dependent on the protein-electrode distance. This last regime is well described by a non-adiabatic electron transfer mechanism, where the ET rate is controlled by the electron tunneling frequency at the top of the activation barrier.⁵⁻¹⁵ However, the nature of the rate-limiting event is more ambiguous for the distance-independent kinetic regime, for which two alternatives have been purported in the literature. The first assumes that, as a consequence of the increased electronic coupling at short protein-electrode distances, the ET rate is controlled by a frictional mechanism that involves the protein and its surrounding medium and takes the reactant to the top of the activation barrier.¹⁶⁻³¹ The second introduces a preceding barrier-crossing event (gating step), which may involve a conformational fluctuation³² or a protein reorientation,³³ to optimize the rate of electron transfer.³²⁻³⁹ Irrespective of the precise nature of the controlling event in the distance-independent kinetic regime, the transition between the two kinetic regimes has been demonstrated by varying systematically the strength of the electronic coupling between electrode and protein by using molecular spacers of variable composition and length. For redox proteins immobilized on thiol monolayers (HS-(CH₂)_n-X) the mechanism transition has often been reported to take place for protein-electrode distance corresponding to $n \approx 10$.^{12, 15, 24, 25, 31, 33, 39-43} Moreover, each kinetic regime can be further characterized by a distinct dependence of the ET rate constant with temperature and solution viscosity,^{25-33, 44, 45} though temperature or viscosity driven mechanism transitions have not yet

1
2
3 been reported for metallo-proteins. To the best of our knowledge, the current work provides the
4
5 first observation of a temperature-induced mechanism changeover for a redox metallo-protein.
6
7

8 Thermal studies of typical redox proteins are significantly restrained, since proteins become
9
10 often denatured at moderate temperatures. A general approach to overcome this limitation would
11
12 involve the use of thermophilic proteins that are likely to keep their structure and functionality
13
14 intact in a broad temperature range. Within this context, we have previously reported on how
15
16 Plastocyanin from *Phormidium laminosum* (Pc-PhoWT) adsorbed onto a graphite electrode
17
18 displays an unusual thermal resistance, retaining its redox activity at temperatures as high as
19
20 90°C.⁴⁶ Pc-PhoWT is a blue copper protein with a Type I redox center. The metal atom is buried
21
22 in a hydrophobic pocket and it is coordinated by two histidines (HisN and HisC), one methionine
23
24 and one cysteine. The Cu binding site features a distorted trigonal pyramid and HisC is the only
25
26 solvent-exposed copper-ligand, thus making this group the most probable physiological electron
27
28 transfer port of the protein (see Supporting Information). Its thermostability has also been probed
29
30 by spectroscopic techniques in a broad temperature range.^{47, 48} Based on these findings, this
31
32 protein appears to be a good candidate to assess the influence of temperature on its ET kinetics.
33
34 Herein, we report on the effect of a broad variation of temperature (0 -90 °C) on the electron
35
36 transfer kinetics of Pc-PhoWT immobilized on gold electrodes modified with 1, ω -alkanedithiol
37
38 self-assembled monolayers (SAMs), under variable conditions of protein-electrode distance and
39
40 solution viscosity. We provide clear experimental evidence of a changeover in the electron
41
42 transfer regime along a thermal scan when Pc-PhoWT is immobilized on a 1,11-undecanedithiol
43
44 monolayer. In this case, electron exchange proceeds through the distance-independent kinetic
45
46 limit at low temperatures, and it switches reversibly into the non-adiabatic regime as the
47
48 temperature is raised over 40 °C.
49
50
51
52
53
54
55
56
57
58
59
60

1
2
3 The redox properties of Pc-PhoWT immobilized on distinct 1, ω -alkanedithiol SAMs differing
4 in their hydrocarbon chain length were characterized by recording its voltammetric response as a
5 function of scan rate. Figure S-2 illustrates some typical raw voltammograms. The formal
6 potential (E^0) shifts from 0.421 V to 0.375 V vs. SHE upon increasing the dithiol chain length,
7 remaining somewhat more positive than the reported values for Pc-PhoWT adsorbed onto
8 graphite⁴⁶ and in solution.⁴⁸ A parallel variation of the reduction entropy (see Supporting
9 Information) towards less negative values suggests that the E^0 shift results from a tighter
10 hydrophobic interaction between protein and monolayer as the alkanedithiol chain-length
11 increases. To determine the standard electron transfer rate constant (k_{ET}^0), the effect of the scan
12 rate on the peak potential separation was assessed at distinct temperatures and electrode-protein
13 distances. Accordingly, upon increasing the scan rate, the two voltammetric peaks depart from
14 each other, producing trumpet plots as those depicted in Figure S-2. Solid lines in these plots are
15 theoretical fits computed in the high reorganization energy limit of the Marcus electron transfer
16 theory (i.e. for $\lambda > F |E_p - E^0|$, where λ is the reorganization energy, E_p the peak potential, and F
17 the Faraday's constant).⁹ Though significant protein loss (ca. 50 %) was evident after exposing
18 the electrode to the hottest solutions, a full recovery of the initial kinetic and thermodynamic
19 electron transfer parameters (see Supporting Information) was observed after subjecting the
20 immobilized protein to broad changes of temperature and solvent viscosity.

21
22
23
24
25
26
27
28
29
30
31
32
33
34
35
36
37
38
39
40
41
42
43
44
45
46
47 The effect of the electrode-protein distance on k_{ET}^0 at distinct temperatures is illustrated in
48 Figure 1. At a given temperature (Figure 1a), it displays a biphasic behavior: the standard
49 electron transfer rate constant barely depends on the chain length up to ca. 9 methylene units, but
50 decays exponentially for the longer chain lengths ($n \geq 11$). The exponential decay factor is
51 $\beta = 1.14$ per methylene group, consistent with the use of saturated hydrocarbon spacers.^{49,50}

Furthermore, Figure 1b shows that the temperature dependence of k_{ET}^0 is stronger at the plateau than within the exponential decay region.

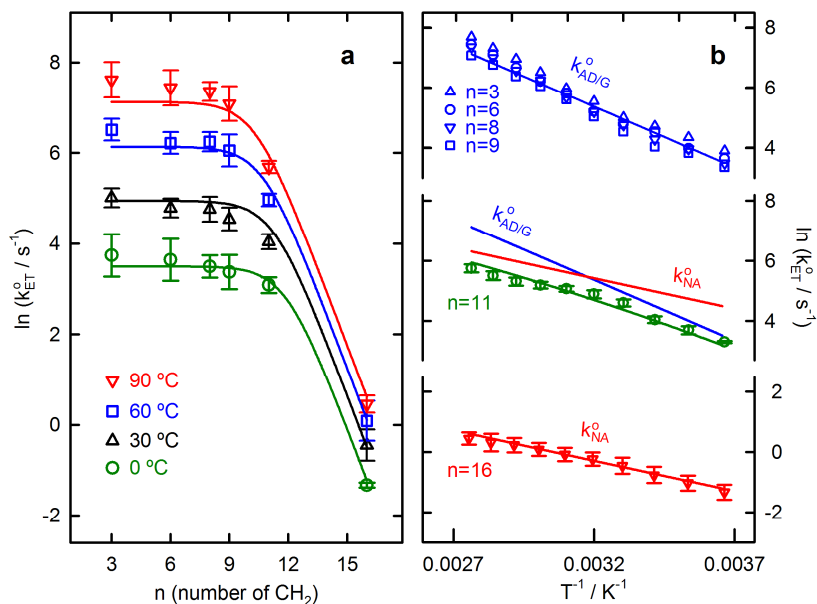


Figure 1. (a) Dependence of the logarithm of the standard electron transfer rate constant on the number of methylene groups per thiol molecule for Pc-PhoWT immobilized on 1,ω-alkanedithiol SAMs, obtained in a 0.1 M sodium phosphate buffer of pH 7 at the indicated temperatures. Solid lines have been computed from eqs 1-4 in the text. (b) Arrhenius plots in the 0 - 90 °C temperature range. The green line in the $n = 11$ plot was computed from the corresponding red and blue lines according to eq 4, as indicated in the text. Symbols are experimental values, and error bars are standard deviations for at least three replicated measurements for each data point.

In the non-adiabatic limit (distance-dependent regime), the standard rate constant k_{ET}^0 is limited by the electron tunneling probability and can be expressed as:

$$k_{NA}^0 = \frac{|H_{AB}^o|^2 \rho_m}{\hbar} \left(\frac{\pi^3 R}{\lambda} \right)^{1/2} \sqrt{T} \exp(-\beta n) \exp\left(-\frac{\lambda/4}{RT}\right) \quad (1)$$

where H_{AB}^o is the electronic coupling energy for $n = 0$ and ρ_m is the density of electronic states of the metal. Fit of eq 1 to experimental $\ln k_{ET}^o$ vs. T^{-1} data for $n = 16$ with $\beta = 1.14$ and $\rho_m = 0.28 \text{ eV}^{-1}$,²⁵ gives rise to $\lambda = 61.7 \text{ kJ mol}^{-1}$ (or 0.64 eV) and $H_{AB}^o = 7 \times 10^{-3} \text{ eV}$. The obtained value for λ falls within the range of accepted values for blue copper proteins.^{46, 51-54}

On the other hand, the standard rate constant under the distance-independent regime can be expressed as:

$$k_{AD}^0 = \frac{1}{\tau_{eff}^o} \left(\frac{\lambda}{\pi^3 R} \right)^{1/2} \frac{1}{\sqrt{T}} \exp\left(-\frac{(\lambda/4) - |H_{AB}^o| e^{-\beta n} + \Delta H_{\eta}^{\#}}{RT}\right) \quad (2)$$

when the electron transfer kinetics are controlled by a frictional mechanism, or simply as:

$$k_G^0 = A_G \exp\left(-\frac{\Delta H_G^{\#}}{RT}\right) \quad (3)$$

when they are controlled by a gating step. τ_{eff}^o is the high-temperature limit of the characteristic polarization relaxation time of the solvent/protein/SAM environment, $\Delta H_{\eta}^{\#}$ is the activation enthalpy associated with solvent/protein/SAM friction, and A_G , $\Delta H_G^{\#}$ are the Arrhenius preexponential factor and height of the activation barrier of the gating step, respectively.

Fit of eq 2 or 3 to the experimental $\ln k_{ET}^o$ vs. T^{-1} data for $n \leq 9$ (Figure 1b) gives rise to $\tau_{eff}^o = 7 \times 10^{-9} \text{ s}$ and $\Delta H_{\eta}^{\#} = 19.1 \text{ kJ mol}^{-1}$ or $A_G = 1.2 \times 10^8 \text{ s}^{-1}$ and $\Delta H_G^{\#} = 34.5 \text{ kJ mol}^{-1}$, respectively. Bearing in mind that $\tau_{eff} = \tau_{eff}^o \exp(\Delta H_{\eta}^{\#} / RT)$, τ_{eff} shows a tenfold decrease from $\sim 32 \mu\text{s}$ at $0 \text{ }^{\circ}\text{C}$ to $\sim 3.9 \mu\text{s}$ at $90 \text{ }^{\circ}\text{C}$. The magnitude of these relaxation times is much larger than those of typical liquids,⁵⁵ and c.a. tenfold the characteristic relaxation time reported by

1
2
3 Khoshtariya et al.²⁵ for the adiabatic electron transfer of cytochrome *c* adsorbed on thiol
4 monolayers. On the other hand, this $\sim 10 \mu\text{s}$ time scale lies well within the $1 - 10^3 \mu\text{s}$ range that
5 has been determined⁵⁶ for the mobility of the $\beta_7 - \beta_8$ loop of the Plastocyanin from *Anabaena*
6 *variabilis*. It should be noted that this loop contains three of the four copper ligands and,
7 therefore, seems to be relevant for the electron transfer process.
8
9

10
11 When the protein is adsorbed on a SAM with an intermediate alkyl chain length ($n = 11$), the
12 $\ln k_{ET}^o$ vs. T^{-1} slope changes from that characteristic of the distance-independent regime, at low
13 temperatures, to that of the non-adiabatic regime at high temperatures. This transition can be
14 accounted for with the following series combination of k_{NA}^o and $k_{AD/G}^o$ (green solid line in Figure
15 1b):
16
17

$$\frac{1}{k_{ET}^o} = \frac{1}{k_{NA}^o} + \frac{1}{k_{AD/G}^o} \quad (4)$$

18
19 which is known to describe the transition from the non-adiabatic to the adiabatic kinetic
20 regimes,²⁵ but it can also account for the presence of a gating step³² (see Supporting
21 Information). As the crossing point of the two individual k_{NA}^o and $k_{AD/G}^o$ contributions to k_{ET}^o
22 shows (Figure 1b), the transition between the two limiting kinetic regimes takes place at ca.
23 40 °C for the $n = 11$ monolayer. It should be noted that this transition is predicted to be outside
24 the available temperature range for $n < 11$ or $n > 11$ (Figure S-7 in Supporting Information).
25
26

27
28 As a test of consistency, eq 4 was able to reproduce the experimental $\ln k_{ET}^o$ vs. n dependence
29 in Figure 1a with the same parameter values that were determined from the analysis of Figure 1b.
30
31

32
33 In order to corroborate the temperature-induced mechanistic changeover found for Pc-PhoWT
34 adsorbed on the $n = 11$ SAM, use was made of the distinct sensitivity of the non-adiabatic and
35 distance-independent kinetic regimes to changes in the solution viscosity η . Previous studies
36
37
38
39
40
41
42
43
44
45
46
47
48
49
50
51
52
53
54
55
56
57
58
59
60

have shown that k_{NA}^o is independent of η , while $k_{AD/G}^o$ is proportional to $\eta^{-\gamma}$ where $\gamma > 0$.^{25, 33, 57}

Thus, according to eq 4, k_{ET}^o is expected to be proportional to $\eta^{-\gamma_{ap}}$, where the value of the γ_{ap} exponent ($0 < \gamma_{ap} \leq \gamma$) depends on the relative contributions of k_{NA}^o and $k_{AD/G}^o$ to k_{ET}^o .

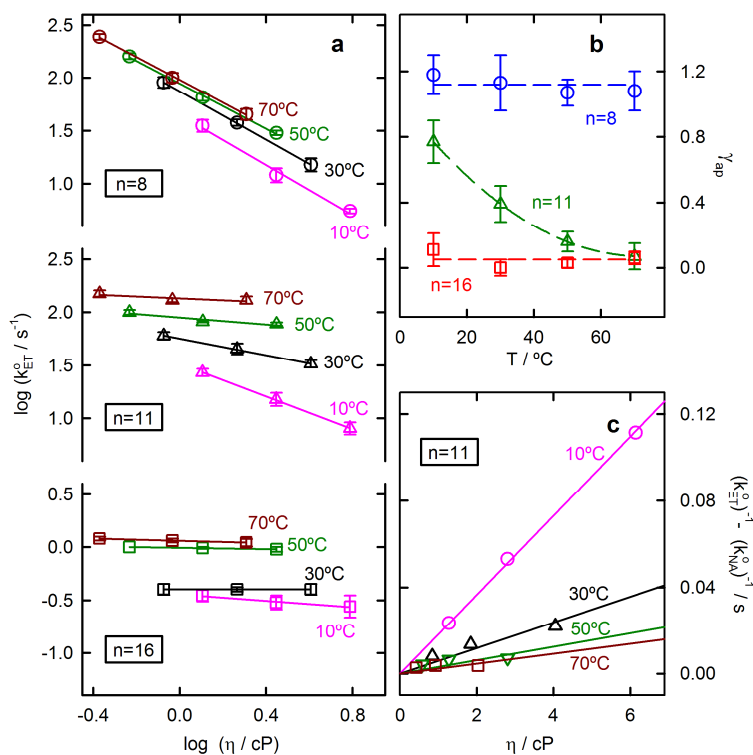


Figure 2. (a) Double logarithmic plot of the overall standard electron transfer rate constant for Pc-PhoWT immobilized on 1, ω -alkanedithiol SAMs, obtained in a 0.1 M sodium phosphate buffer of pH 7, against solution viscosity for the indicated temperature and spacer's number of methylene groups. (b) Slopes of the $\log k_{ET}^o$ vs. $\log \eta$ plots in Figure 2a as a function of temperature. (c) Difference between the reciprocals of the observed and calculated non-adiabatic standard electron transfer rate constants as a function of solution viscosity for $n = 11$ and the indicated temperatures. Solid lines are least squares linear fits passing through the origin.

Figure 2a illustrates the observed dependence of k_{ET}^0 on the viscosity of aqueous glucose solutions, under variable conditions of electrode-protein distance and temperature. It can be observed that the slope of the logarithmic plot (i.e. γ_{ap}) decreases upon increasing the SAM thickness, from $\gamma_{ap} \approx 1.1$ for $n = 8$ to $\gamma_{ap} \approx 0.0$ for $n = 16$, in agreement with the change of kinetic regime discussed previously. More importantly, the slopes corresponding to the intermediate $n = 11$ SAM display a continuous variation with temperature from $\gamma_{ap} = 0.77$ at 10°C to $\gamma_{ap} = 0.09$ at 70°C (Figure 2b), as expected for a changeover of the electron transfer mechanism from the frictional/gating regime to the non-adiabatic one. In order to quantify the γ value, corresponding to the $k_{AD/G}^0$ term, we have plotted in Figure 2c the difference between observed $1/k_{ET}^0$ and calculated $1/k_{NA}^0$, as a function of solution viscosity, where the k_{NA}^0 values have been computed from eq 1 with the parameter values determined previously. According to eq 4, the ordinate values in these plots correspond to those of $1/k_{AD/G}^0$. The linearity of these plots strongly suggests that the frictional coupling to the medium is very strong, with a real γ value close to 1.

Previous reports describing the transition between frictional/gating and non-adiabatic electron transfer mechanisms for immobilized cytochrome c^{25} and azurin³¹ took advantage of the high sensitivity of the non-adiabatic electron transfer rate to the electrode-protein distance. Herein, we have shown that the same transition can be achieved by exploiting the difference in the activation enthalpies of these two mechanisms. Once an adequate tunneling distance is selected, so that the values of the frictional/gating and non-adiabatic rate constants become similar at intermediate temperatures, the kinetic control can then be switched reversibly between the frictional/gating and non-adiabatic limits by just varying the temperature. In the case of the thermophilic

1
2
3 plastocyanin from *Phormidium laminosum* adsorbed on a 1,11-undecanedithiol SAM, the
4
5 mechanistic changeover takes place at 40 °C. This transition results from the interplay between
6
7 different contributions to the observed ET rate, and our previous analysis helps to identify some
8
9 physical prerequisites, such as the necessary difference in activation enthalpy between the two
10
11 kinetic regimes or the importance of an adequate choice of the tunneling distance, to observe
12
13 similar transitions for other redox proteins.
14
15
16
17
18
19
20

21 ASSOCIATED CONTENT

22 23 24 **Supporting information**

25
26
27 Experimental Method, Materials and Methods. Structure of Plastocyanin from *Phormidium*
28
29 *laminosum*. Typical Cyclic Voltammograms and Trumpet Plots. Thermal Stability of the SAM
30
31 and the Immobilized Pc-PhoWT. Expressions for the Rate Constants. Individual Contributions to
32
33 the Electron Transfer Rate Constant. Thermodynamics of the Immobilized Pc-PhoWT. This
34
35 material is available free of charge via the Internet at <http://pubs.acs.org>.
36
37
38
39

40 AUTHOR INFORMATION

41 42 43 **Corresponding Author**

44
45
46 *Email: jlolloqui@us.es
47
48

49 **Notes**

50
51
52 The authors declare no competing financial interests.
53
54
55
56
57
58
59
60

ACKNOWLEDGMENT

J. L. O., J. J. C. and R. A. acknowledge financial support from the DGICYT under grant CTQ 2008-00371 and from the Junta de Andalucía under grant P07-FQM-02492. B. M. B., A. D. Q. and M. A. R. recognize funding grant P06-CVI-01713 from Junta de Andalucía and DGICYT (BFU2012-31670/BMC). B.M.B Ph.D. fellowship from the M.E.C.D. (AP2009/4092) is co-funded by the E.S.F.-E.R.F.

REFERENCES

- (1) Fedurco, M. Redox Reactions of Heme-Containing Metalloproteins: Dynamic Effects of Self-Assembled Monolayers on Thermodynamics and Kinetics of Cytochrome *c* Electron-Transfer Reactions. *Coor. Chem. Rev.* **2000**, 209, 263-331.
- (2) Armstrong, F. A.; Wilson, G. S. Recent Development in Faradaic Bioelectrochemistry. *Electrochim. Acta* **2000**, 45, 2623-2645.
- (3) Jeuken, L. J. C. Conformational Reorganisation in Interfacial Protein Electron Transfer *Biochim. Biophys. Acta* **2003**, 1604, 67-76.
- (4) Murgida, D. H.; Hildebrandt, P. Redox and Redox-Coupled Processes of Heme Proteins and Enzymes at Electrochemical Interfaces *Phys. Chem. Chem. Phys.* **2005**, 7, 3773-3784.
- (5) Waldeck, D. H.; Khoshtariya, D. E. in *Modern Aspects of Electrochemistry. Applications of Electrochemistry and Nanotechnology in Biology and Medicine*. Ed. Elias; Springer, New York **2011**, 52, 105-238.
- (6) Hopfield, J. J. Electron Transfer between Biological Molecules by Thermally Activated Tunneling. *Proc. Natl. Acad. Sci. USA* **1974**, 71, 3640-3644.
- (7) Marcus, R. A.; Sutin, A. N. Electron Transfer in Chemistry and Biology. *Biochim. Biophys. Acta* **1985**, 811, 265-322.

- 1
2
3
4 (8) Chidsey, C. E. D. Free Energy and Temperature Dependence of Electron Transfer at the
5 Metal-Electrolyte Interface. *Science* **1991**, 251, 919-922.
6
7
8 (9) Weber, K.; Creager, S. E. Voltammetry of Redox-Active Groups Irreversibly Adsorbed
9 onto Electrodes. Treatment using Marcus Relation between Rate and Overpotential. *Anal.*
10 *Chem.* **1994**, 66, 3164-3172.
11
12
13 (10) Kuznetsov, A. M.; Ulstrup J. *Electron Transfer in Chemistry and Biology* (Wiley
14 Chichester, UK) **1999**, 1-374.
15
16
17 (11) Smalley, J. F.; Feldberg, S. W.; Chidsey, C. E. D.; Lindford, M. R.; Newton, M. D.;
18 Liu, Y. P. The Kinetics of Electron Transfer through Ferrocene-Terminated Alkanethiol
19 Monolayers on Gold. *J. Phys. Chem.* **1995**, 13141-13149.
20
21
22 (12) Chi, Q.; Zhang, J.; Andersen, J. E. T.; Ulstrup, J. Ordered Assembly and Controlled
23 Electron transfer of the Blue Copper Protein Azurin at Gold (111) Single-Crystal
24 Substrates. *J. Phys. Chem. B* **2001**, 105, 4669-4679.
25
26
27 (13) Gray, H. B.; Winkler, J. R. Electron Tunneling through Proteins. *Quart. Rev Biophys.*
28 **2003**, 36, 341-372.
29
30
31 (14) Feldberg, S. W.; Sutin, N. Distance Dependence of Heterogeneous Electron Transfer
32 through the Nonadiabatic and Adiabatic Regimes. *Chem. Phys.* **2006**, 324, 216-225.
33
34
35 (15) Yokoyama, K.; Leigh, B. S.; Sheng, Y.; Niki, K.; Nakamura, N.; Ohno, H.; Winkler, J.
36 R.; Gray, H. B.; Richards, J. H. Electron Tunneling through *Pseudomonas aureginosa*
37 Azurins on SAM Gold Electrodes. *Inorg. Chim. Acta* **2008**, 361, 1095-1099.
38
39
40 (16) Zusman, L. D. Outer-Sphere Electron Transfer in Polar Solvents. *Chem. Phys.* **1980**, 49,
41 295-304.
42
43
44 (17) Zusman, L. D. The Theory of Transitions between Electronic States: Application to
45 Radiationless Transition in Polar Solvents. *Chem. Phys.* **1983**, 80, 29-43.
46
47
48
49
50
51
52
53
54
55
56
57
58
59
60

- 1
2
3
4
5
6
7
8
9
10
11
12
13
14
15
16
17
18
19
20
21
22
23
24
25
26
27
28
29
30
31
32
33
34
35
36
37
38
39
40
41
42
43
44
45
46
47
48
49
50
51
52
53
54
55
56
57
58
59
60
- (18) Rips, I.; Jortner, J. Dynamic Solvent Effects on Outersphere Electron Transfer. *J. Chem. Phys.* **1987**, 87, 2090-2104.
- (19) Beratan, D. N.; Onuchic, J. N. Adiabacity and Non-Adiabacity in Bimolecular Outer-Sphere Charge Transfer Reaction. *J. Chem. Phys.* **1988**, 89, 6195-6203.
- (20) Weaver, M. J.; Mac-Manis, G. E. Dynamical Solvent Effects on Electron-Transfer Processes: Recent Progress and Perspectives. *Acc. Chem. Res.* **1990**, 23, 294-300
- (21) Weaver, M. J. Dynamical Solvent Effects on Activated Electron-Transfer Reactions: Principles, Pitfalls and Progress. *Chem. Rev.* **1992**, 92, 463-480.
- (22) Zusman, L. D. Dynamical Solvent Effect in Electron Transfer Reaction. *Z. Phys. Chem.* **1994**, 186, 1-29.
- (23) Khoshtariya, D. E.; Dolidze, T. D.; Zusman, L.D.; Waldeck, D.H. Observation of the Turnover between the Solvent Friction (Overdamped) and Tunneling (Nonadiabatic) Charge-Transfer Mechanisms for a Au/Fe(CN)₆^{3-/4-} Electrode Process and Evidence for a Freezing out of the Marcus Barrier. *J. Phys. Chem. A* **2001**, 105, 1818-1829.
- (24) Wei, J.; Liu, H.; Khoshtariya, D. E.; Yamamoto, H.; Dick, A.; Waldeck, D. H. Electron-Transfer Dynamics of Cytochrome C: A Change in the Reaction Mechanism with Distance. *Angew. Chem. Int. Ed.* **2002**, 41, 4700-4703.
- (25) Schmickler, W.; Mohr, J. The Rate of Electrochemical Electron-Transfer Reactions. *J. Chem. Phys.* **2002**, 117, 2867-2872.
- (26) Khoshtariya, D. E.; Wei, J.; Liu, H.; Yue, H.; Waldeck, D. H. Charge-Transfer Mechanism for Cytochrome C Adsorbed in Nanometer Thick Films. Distinguishing Frictional Control from Conformational Gating. *J. Am. Chem. Soc.* **2003**, 125, 7704-7714.
- (27) Khoshtariya, D. E.; Dolidze, T. D.; Sarauli, D.; Van Eldik, R. High-Pressure Probing of a Changeover in the Charge-Transfer Mechanism for Intact Cytochrome *c* at Gold/Self-Assembled Monolayers Junctions. *Angew. Chem. Int. Ed.* **2006**, 45, 277-281.

- 1
2
3 (28) Yue, H.; Khoshtariya, D. E.; Waldeck, D.H.; Grochol, J; Hildebrandt, P.; Murgida, D.H.
4 On the Electron Transfer Mechanism Between Cytochrome *C* and Metal Electrodes.
5 Evidences for Dynamic Control at Short Distances. *J. Phys. Chem. B* **2006**, 110, 19906-
6 19913.
7
8
9
10
11 (29) Mishra, A. K.; Waldeck, D. H. A Unified Model for the Electrochemical Rate Constant
12 that Incorporates Solvent Dynamics. *J. Phys. Chem. C* **2009**, 113, 17904-17914.
13
14
15
16 (30) Khoshtariya, D. E.; Dolidze T. D.; Van Eldik, R. Multiple Mechanisms for Electron
17 Transfer at Metal/Self-Assembled Monolayer/Room-Temperature Ionic Liquid Junctions:
18 Dynamical Arrest versus Frictional Control and Non-Adiabaticity. *Chem. Eur. J.* **2009**,
19 15, 5254-5262.
20
21
22
23
24 (31) Khoshtariya, D. E.; Dolidze, T. D.; Shushanyan, M.; Davis, K. L.; Waldeck, D.H.; Van
25 Eldik, R. Fundamental Signatures of Short- and Long-Rate Electron Transfer for the Blue
26 Copper Protein Azurin at Au/SAM Junction. *Proc. Natl. Acad. Sci. USA* **2010**, 107, 2757-
27 2762.
28
29
30
31
32 (32) Sumi, H. Theory on Reaction Rates in Nonthermalized Steady States during
33 Conformational Fluctuations in Viscous Solvents. *J. Phys. Chem.* **1991**, 95, 3334-3350.
34
35
36
37 (33) Avila, A.; Gregory, B. W.; Niki, K.; Cotton, T. M. An Electrochemical Approach to
38 Investigate Gated Electron Transfer using a Physiological Model System: Cytochrome *c*
39 Immobilized on Carboxylic Acid-Terminated Alkanethiol Self-Assembled Monolayers
40 on Gold Electrodes. *J. Phys. Chem. B* **2000**, 104, 2759-2766
41
42
43
44
45 (34) Davidson, V. Protein Control of True, Gated and Coupled Electron Transfer Reactions.
46 *Acc. Chem. Res.* **2008**, 41, 730-738.
47
48
49
50 (35) Kranich, A.; Ly, H. K.; Hildebrandt, P.; Murgida, D. H. Direct Observation of the
51 Gating Step in Protein Electron Transfer: Electric-Field-Controlled Protein Dynamics. *J.*
52 *Am. Chem. Soc.* **2008**, 130, 9844-9848.
53
54
55
56 (36) Kranich, A.; Naumann, H.; Molina-Heredia, F. P.; Moore, H. J.; Lee, T. R.; Lecomte,
57 S.; De la Rosa, M. A.; Hildebrandt, P.; Murgida D. H. Gated Electron Transfer of
58
59
60

1
2
3
4
5
6
7
8
9
10
11
12
13
14
15
16
17
18
19
20
21
22
23
24
25
26
27
28
29
30
31
32
33
34
35
36
37
38
39
40
41
42
43
44
45
46
47
48
49
50
51
52
53
54
55
56
57
58
59
60

Cytochrome *c*₆ at Biomimetic Interfaces: A Time-Resolved SERR Study. *Phys. Chem. Chem. Phys.* **2009**, 11, 7390-7397.

(37) Álvarez-Paggi, D.; Martin, D. F.; DeBiase, P. M.; Tenger, K.; Hildebrandt, P.; Martí, M. A.; Murgida, D. H. Molecular Basis of Coupled Protein and Electron Transfer Dynamics of Cytochrome *c* in Biomimetic Complexes. *J. Am. Chem. Soc.* **2010**, 132, 5769-5778.

(38) Georg, S.; Kabuss, J.; Weidinger, I. M.; Murgida, D. H.; Hildebrandt, P.; Knorr, A.; Richter, M. Distance-Dependent Electron Transfer of Immobilized Redox Protein: A Statistical Physics Approach. *Phys. Rev. E* **2010**, 81, 046101/1-046101/10.

(39) Álvarez-Paggi, D.; Meister, W.; Kuhlmann, U.; Weidinger, I.; Tenger, K.; Zimányi, L.; Rákhely, G.; Hildebrandt, P.; Murgida, D. H. Distangling Electron Tunneling and Protein Dynamics of Cytochrome *C* through a Rationally Designed Surface Mutation. *J. Phys. Chem. B* **2013**, 117, 6061-6068.

(40) Liu, H.; Yamamoto, H.; Wei, J.; Waldeck, D. H. Control of the Electron Transfer Rate between Cytochrome *c* and Gold Electrodes by the Manipulation of the Electrode's Hydrogen Bonding Character. *Langmuir* **2003**, 2378-2387.

(41) Davis, K. L.; Drews, B. J.; Yue, H.; Waldeck, D. H.; Knorr, K.; Clark, L. A. Electron Transfer Kinetics of Covalently Attached Cytochrome *c*/SAM/Au Electrode Assemblies. *J. Phys. Chem. C* **2008**, 7, 3773-3784.

(42) Monari, S.; Battistuzzi, G.; Dennison, C.; Borsari, M.; Ranieri, A.; Siwek, J. M.; Sola, M. Factors Affecting the Electron Transfer Properties of Immobilized Cupredoxin. *J. Phys. Chem. C* **2010**, 114, 22322-22329.

(43) Monari, S.; Battistuzzi, G.; Bortolotti, C. A.; Yanagisawa, S.; Sato, K.; Li, C.; Salard, I.; Kostrz, D.; Borsari, M.; Ranieri, A.; Dennison, C.; Sola, M. Understanding the Mechanism of Short-Range Electron Transfer using an Immobilized Cupredoxin. *J. Am. Chem. Soc.* **2012**, 134, 11848-11851.

- 1
2
3
4 (44) Harris, M. R.; Davis, D. J.; Durham, B.; Millet, F. Temperature and Viscosity
5 Dependence of the Electron-Transfer Reaction between Plastocyanin and Cytochrome *c*
6 Labeled with a Ruthenium (II) Bipyridine Complex. *Biochim. Biophys. Acta* **1997**, 1319,
7 147-145.
8
9
10
11 (45) Khoshtariya, D. E.; Dolidze, T. D.; Seifert, S.; Sarauli, D.; Lee, G.; Van Eldik, R.
12 Kinetic, Thermodynamic, and Mechanistic Patterns for Free (Unbound) Cytochrome *c* at
13 Au/SAM Junctions: Impact of Electronic Coupling, Hydrostatic Pressure, and
14 Stabilizing/Denaturing Additives. *Chem. Eur. J.* **2006**, 12, 7041-7056.
15
16
17
18 (46) Olloqui-Sariego, J. L.; Frutos-Beltrán, E.; Roldán, E.; De la Rosa, M. A.; Calvente, J. J.;
19 Díaz-Quintana, A.; Andreu, R. Voltammetric Study of the Adsorbed Thermophilic
20 Plastocyanin from *Phormidium laminosum* up to 90°C. *Electrochem. Commun.* **2012**, 19,
21 105-107.
22
23
24
25
26
27 (47) Feio, M. J.; Navarro, J. A.; Teixeira, M. S.; Harrison, D.; Karlsson, B. G.; De la Rosa,
28 M. A. A Thermal Unfolding Study of Plastocyanin from the Thermophilic
29 Cyanobacterium *Phormidium laminosum*. *Biochemistry* **2004**, 43, 14784–14791.
30
31
32
33 (48) Muñoz-López, F. J.; Frutos-Beltrán, E.; Díaz-Moreno, S.; Díaz-Moreno, I.; Subías, G;
34 De la Rosa, M. A.; Díaz-Quintana, A. Modulation of Copper Site Properties by Remote
35 Residues Determines the Stability of Plastocyanins. *FEBS Lett.* **2010**, 584, 2346–2350.
36
37
38
39 (49) Oevering, H.; Paddon-Row, M. N.; Heppener, M.; Oliver, A. M.; Cotsaris, E.;
40 Verhoeven, J. W.; Hush, N. S. Long-Range Photoinduced Through-Bond Electron
41 Transfer and Radiative Recombination via Rigid Nonconjugated Bridges: Distance and
42 Solvent Dependence. *J. Am. Chem. Soc.* **1987**, 109, 3258-3269.
43
44
45
46
47 (50) Smalley, J. F.; Frinklea, H. O.; Chidsey, C. E. D.; Linford, M. R.; Creager, S. E.;
48 Ferraris, J. P.; Chalfant, K.; Zawodzinsk, T.; Feldberg, S. W.; Newton, M. D.
49 Heterogeneous Electron Transfer Kinetics Ruthenium and Ferrocene Redox Moieties
50 through Alkanethiol Monolayers on Gold. *J. Am. Chem. Soc.* **2003**, 125, 2004-2013.
51
52
53
54
55
56
57
58
59
60

- 1
2
3
4
5
6
7
8
9
10
11
12
13
14
15
16
17
18
19
20
21
22
23
24
25
26
27
28
29
30
31
32
33
34
35
36
37
38
39
40
41
42
43
44
45
46
47
48
49
50
51
52
53
54
55
56
57
58
59
60
- (51) Di Bilio, A. J.; Hill, M. G.; Bonander, N.; Karlsson, B. G.; Villahermosa, R. M.; Malmström, B. G.; Winkler, J. R.; Gray, H. B. Reorganization Energy of Blue Copper: Effects of Temperature and Driving Force on the Rates of Electron Transfer in Ruthenium-Osmium-Modified Azurins. *J. Am. Chem. Soc.* **1997**, 119, 9921-9922.
- (52) Solomon, E. I.; Szilagyi, R. K.; DeBeer-George, S.; Basumallick, L. Electronic Structures of Metal Sites in Protein and Models: Contributions to Function in Blue Copper Proteins. *Chem. Rev.* **2004**, 104, 419-458.
- (53) Cascella, M.; Magistrato, A.; Tavernelli, I.; Carloni, P.; Rothlisberger, U. Role of the Protein Frame and Solvent for the Redox Properties of Azurin from *Pseudomonas aureginosa*. *Proc. Natl. Acad. Sci. USA* **2006**, 103, 19641-19646.
- (54) LeBard, D. N.; Matyushov, D. V. Glassy Protein Dynamics and Gigantic Solvent Reorganization Energy of Plastocyanin. *J. Phys. Chem. B* **2008**, 112, 5218-5227.
- (55) Fawcet, W. R. Liquids, Solutions and Interfaces, *Oxford University Press*, New York, **2004**.
- (56) Ma, L.; Hass, M. A. S.; Vierick, N.; Kristenses, S. N.; Ulstrup, J.; Led, J. J. Backbones Dynamics of Reduced Plastocyanin from Cyanobacterium *Anabaena Variabilis*: Regions Involved in Electron Transfer Have Enhanced Mobility. *Biochemistry* **2003**, 42, 320-330.
- (57) Zhou, J. S.; Kostic, N. M. Gating of Photoinduced Electron Transfer from Zinc Cytochrome *c* and Tin Cytochrome *c* to Plastocyanin. Effects of Solution Viscosity on Rearrangement of the Metalloprotein Complex. *J. Am. Chem. Soc.* **1993**, 115, 10796-10804.